DESY 16-005
APCTP Pre2016-003
January 22, 2016

Testing ATLAS Z+MET Excess with LHC Run 2

Xiaochuan Lu[(a)], **Satoshi Shirai**[(b)] and **Takahiro Terada**[(c,d)]

[(a)] *Department of Physics, University of California, Davis, California 95616, USA*
[(b)] *Deutsches Elektronen-Synchrotron (DESY), 22607 Hamburg, Germany*
[(c)] *Department of Physics, University of Tokyo, Tokyo 113-0033, Japan*
[(d)] *Asia Pacific Center for Theoretical Physics (APCTP), Pohang, 37673, Korea*

Abstract

The ATLAS collaboration reported a 3σ excess in events containing dilepton on Z, jets, and large missing momentum (MET) in the 8 TeV LHC running. Motivated by this excess, many types of new physics models have been proposed. Recently, the ATLAS and CMS collaborations reported new results for the similar Z+MET channels in the 13 TeV running. In this paper, we comprehensively discuss consistency of the proposed models with both LHC results at Run 1 and Run 2. We find models with heavy gluino production generically have some tension between the 8 TeV and 13 TeV observations, whereas models with light squark production provide relatively better fitting to both results.

1 Introduction

The ATLAS collaboration reported an excess in the search for supersymmetry (SUSY) in events containing an on-Z dilepton with large missing transverse momentum (MET) and jet activity at the 8 TeV running [1]. In this search, 16 (13) events were observed in di-electron (di-muon) signal channel, while the number of the expected Standard Model (SM) background is 4.2 ± 1.6 (6.4 ± 2.2). This reads a 3.0σ deviation from the SM background. If we assume the ATLAS Z+MET excess comes from new physics, the observed *visible cross section*, *i.e.* the cross section σ times the acceptance rate ϵ for the signal selection, is estimated as

$$(\epsilon\sigma)^{\rm NP,obs}_{\rm 8TeV} = 0.9 \pm 0.3 \text{ fb}. \tag{1}$$

Although this excess has yet to be statistically significant to conclude the evidence of new physics, it gathered much attention. Many types of new physics models have been proposed to explain this excess [2–13]. Most of these models are based on SUSY, but some non-SUSY models are also proposed. Generically, these models also predict signal channels other than the dilepton+MET, because Z boson has a branching fraction of hadronic decay much larger than its dilepton decay. For instance, the jets+MET+zero-lepton search is expected to place severe constraints on them. Many proposed models dodge these constraints. Typically, a compressed spectrum is considered, then the jet and MET activities are reduced. This feature is also consistent with the detailed analysis of the ATLAS Z+MET excess — the ATLAS collaboration provides more detailed information on the Z+MET events, distributions of MET, $H_{\rm T}$ (a scalar sum of the transverse momenta of the signal jets and leptons) and jet multiplicity [1]. These detailed information show that lower jet activity is favored, which would be consistent with the negative results of jets+MET+zero-lepton search.

Another subtlety is the Z+MET search by the CMS at Run 1 [14]. The CMS collaboration has an analogous search for events with a dilepton on-Z, jets, and MET. While these channels resemble the ATLAS channels, no excess is found. This fact complicates the situation, and clearer tests are needed to study the ATLAS Z+MET excess. However the event selections of the ATLAS and CMS collaborations at Run 1 are not exactly the same. For instance, no $H_{\rm T}$ cut is required in the CMS analysis. Some models may avoid the CMS constraints, due to the different event selections.

Recently, the ATLAS and CMS collaborations reported the first Run 2 results of the searches for the Z+MET events [15, 16] using data taken in 2015. Although both collaborations use slightly severer lepton selection criteria, they adopt very similar event selections to the ATLAS analysis at Run 1. Interestingly, the ATLAS collaboration still report an excess — in the dilepton channel, 21 events are observed while 10.3 ± 2.3 SM backgrounds are expected, which amounts to 2.2σ excess, but the CMS result is still consistent with the SM background. In Table 1, we summarize the observations by the ATLAS and CMS collaborations.

In this paper, we study the consistency of the new physics models proposed to explain the 8 TeV ATLAS excess with the 13 TeV ATLAS result as well as other constraints like CMS Z+MET searches. This comparison provides robust tests of such models — for certain new physics models, accompanying signals channels such as jets+MET+zero-lepton events, or some other optimized events cut might be more constraining. However, this kind of indirect constraints may be circumvented by tuning some parameters, and hence less robust than a direct comparison of the same channels at 8/13 TeV.

Assuming the excess of ATLAS Run 2 also comes from new physics, the observed visible cross

Table 1: Observations and Background in the Z+MET channel. The distribution of the number of b-jets among the leading three jets is taken from Figure 5.25 of Ref. [17].

	$n_{b\text{-jets}}$	SM background	Observed number	Reference
ATLAS 8 TeV (20.3 fb^{-1})		10.6 ± 3.2	29	[1]
	0	(7.5 ± 1.4)	18	[17]
	1	(4.7 ± 0.5)	8	
	2	(1.5 ± 0.9)	3	
	3	(0)	0	
ATLAS 13 TeV (3.2 fb^{-1})		10.3 ± 2.3	21	[15]
CMS 13 TeV (ATLAS-like) (2.2 fb^{-1})		$12.0^{+4.0}_{-2.8}$	12	[16]

section at ATLAS Run 2 is

$$(\epsilon\sigma)^{\rm NP,obs}_{\rm 13TeV} = 3.3 \pm 1.6 \text{ fb}. \tag{2}$$

We define the observed ratio of the visible cross sections at ATLAS

$$R^{\rm obs} \equiv \frac{(\epsilon\sigma)^{\rm NP,obs}_{\rm 13TeV}}{(\epsilon\sigma)^{\rm NP,obs}_{\rm 8TeV}} = 3.7^{+2.7}_{-1.8}. \tag{3}$$

As we will see later, the predicted values of R from new physics models tend to be larger than the observed value above, and large parameter regions are found disfavored. To understand this, we show in Fig. 1a the ratios of cross sections at 13/8 TeV LHC for typical heavy colored particle productions. In addition, the ratio of acceptance rates $(\epsilon)_{\rm 13TeV}/(\epsilon)_{\rm 8TeV}$ is typically of order 1, as shown in Fig. 1b. In this figure we assume the gluino decay chain $\tilde{g} \to g(X_2 \to ZX_1)$ and the squark decay chain $\tilde{q} \to q(X_2 \to ZX_1)$, where X_1 and X_2 are the lightest supersymmetric particle (LSP) and the next-to-LSP respectively, and $M_{X_2} - M_{X_1} = 100$ GeV. Combining Fig. 1a and 1b, we see that the predicted R value is generically larger than $R^{\rm obs}$. Lower parent particle mass leads to lower values of R. Moreover, in the cases that parent particles are produced by valence quarks (*e.g.* the heavy gluon model or T-channel production of the squarks to be discussed further in the following sections), the R value tends to be small. Therefore, light parent particles and/or production via valence quarks are favored for the best fit of 13/8 TeV ATLAS excesses.

The rest of this paper is organized as follows. We first review the various new physics models proposed to explain the 8 TeV ATLAS Z+MET excess in section 2. Then in section 3, we reduce these models into simplified models and check their consistency with the LHC Run 2. Section 4 is devoted to discussion.

2 Models

To explain the 8 TeV ATLAS Z+MET excess, a new physics model must satisfy the following three conditions:

1. Having a substantial production cross section of the parent particle.
2. The parent particle having a large decay branching fraction into Z bosons.

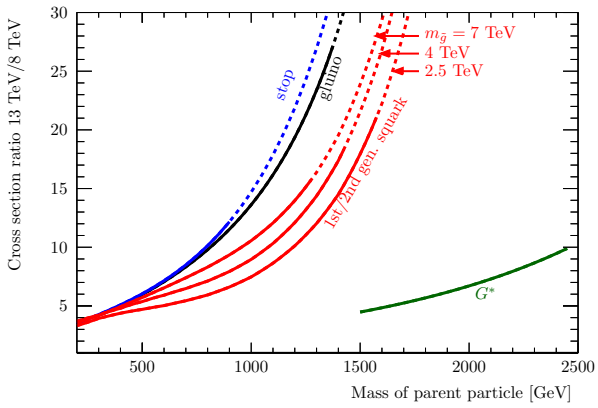

(a) Cross section ratios 13 TeV/ 8TeV.

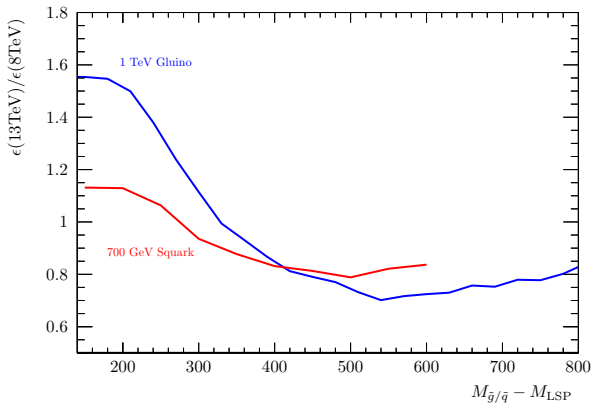

(b) Acceptance ratios 13 TeV/ 8TeV.

Figure 1: (a): The ratio of the cross sections at 13/8 TeV LHC. On the solid lines, the cross sections at $\sqrt{s} = 8$ TeV is greater than 1 fb, which will be the least value to explain the ATLAS8 Z+MET excess. In the case of 1st/2nd generation squark productions, the line gets closer to the stop line as $m_{\tilde{g}} \to \infty$. (b): The ratio of the acceptance rates at 13/8 TeV LHC. The blue (red) line shows the 1 TeV gluino (700 GeV squark) case. Here we assume the gluino decay chain $\tilde{g} \to g(X_2 \to ZX_1)$ and the squark decay chain $\tilde{q} \to q(X_2 \to ZX_1)$, where X_1 (X_2) is the (N)LSP and $M_{X_2} - M_{X_1} = 100$ GeV. See the text for details.

3. Surviving the constraints from searches other than dilepton+MET, such as jets+MET+zero-lepton search.

To satisfy Condition 1, usually strong interaction is assumed as the production mechanism of the parent particle. This is because the electroweak (EW) production requires light parent particles to gain a sufficient cross section, but such a spectrum cannot survive the experimental cuts, in particular the H_{T} cut [2]. However, if the production cross section is too large, a large number of non-dilepton events are also induced, which tends to conflict with Condition 3.

Conditions 1 and 2 together guarantee a substantial production rate of the Z boson, which is needed to explain the Z+MET excess. For this purpose alone, it seems that one could remove Condition 2 while compensating it by further improving Condition 1, i.e. having a larger production cross section of the parent particle. But due to Condition 3, generically this would not work. Therefore, Condition 2 is really crucial in explaining the Z+MET excess. However, in many cases, the $\text{SU}(2)_L$ gauge invariance leads to branching fractions into W bosons or Higgs bosons (h) comparable with that into Z boson, which violates Condition 2.

In order to overcome this problem, the general gauge mediation (GGM) [18, 19] with the neutralino NLSP and a very light gravitino LSP can be considered [2, 3]. Due to the tiny interactions between the SUSY SM particles and gravitino, all the decay chains contain decay of the lightest neutralino into the gravitino. Tuning the parameters of the neutralino sector, the branching fraction of the lightest neutralino into Z boson and gravitino can be enhanced. Nonetheless, because the gravitino LSP is almost massless in this type of models, the jet activity and MET turn out to be large, and Condition 3 gets harder to be satisfied [3]. As we will see, the new physics searches at 13 TeV provides stronger constraints on the GGM. In addition, in both 8 TeV and 13 TeV excesses, the jet activity and momentum of the Z boson are small in the signal regions [1, 15]. If we take

these properties into account seriously, the GGM cases may be disfavored.

Another way of enhancing the branching fraction into Z boson is to have a compressed mass spectrum. If the mass gap between new physics particles is the order of EW scale, we can tune $\mathrm{SU}(2)_L$ breaking masses so that the branching fraction into the Z boson is selectively enhanced. For instance, consider the decay of the second lightest neutralino into the lightest one $\tilde{\chi}_2^0 \to \tilde{\chi}_1^0$. If $M_Z < M_{\tilde{\chi}_2^0} - M_{\tilde{\chi}_1^0} < M_h$, then the branching fraction into Z boson can dominate over that into h. Such a compressed mass spectrum also has an advantage for the Condition 3. Therefore proposed models often contain compressed mass spectra.

In the following, we classify various proposed models explaining the ATLAS Z+MET excess into three categories: (1) SUSY models with gluino production, (2) SUSY models with squark production, and (3) a non-SUSY model. As mentioned above, the EW production is not considered, since it cannot produce enough Z bosons after the experimental cuts.

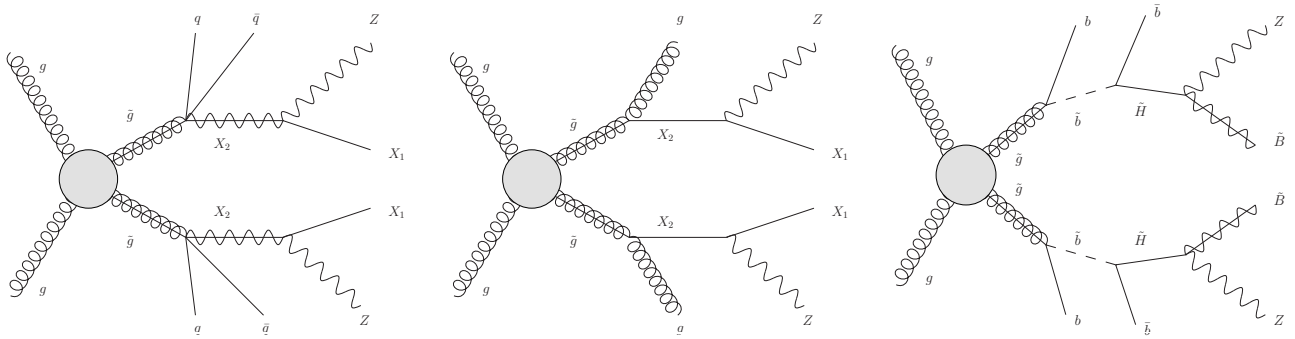

(a) gluino 3-body decay (b) gluino 2-body decay (c) gluino decay via light sbottom

(d) squark pair (e) mixed-stop (f) heavy gluon

Figure 2: Feynman diagrams of typical decay chains emitting Z bosons in models reviewed in section 2. One of the typical production processes is also depicted in each case.

2.1 Gluino production

This category is further divided into subcategories according to the decay of gluino.

Quark-antiquark emission

The first case is that the gluino decaying into a quark-antiquark pair and a neutralino, which subsequently decays into a Z boson and a neutral LSP. This decay chain $\tilde{g} \to q\bar{q}X_2 \to q\bar{q}ZX_1$, with X_1 (X_2) denoting the neutral (N)LSP, is shown in Fig. 2a. In the literature, (1) the GGM model [2, 3] and (2) the NMSSM models with gluino production [4–6] belong to this case. In case (1), $X_2 = \tilde{\chi}_1^0$ (the lightest neutralino) and $X_1 = \tilde{G}$ (the gravitino), and one can tune the SUSY SM parameters so that the branching fraction of $\tilde{\chi}_1^0$ to Z and $\tilde{G}$ is close to 100%. Direct decay of $\tilde{g}$ into $\tilde{G}$ is suppressed due to the tiny interaction between the gravitino and SUSY SM particles. Due to the nearly massless LSP, this case is strongly constrained by jets+MET+zero-lepton search and multi-lepton search at LHC Run 1 [3]. In case (2), $X_2 \simeq \tilde{B}$ [5] or $X_2 \simeq \tilde{H}$ [6] and $X_1 \simeq \tilde{S}$ (the singlino). The small coupling of the singlino suppresses direct decay of the gluino into it, just as in the case of gravitino in the GGM model. In this case, the LSP is massive and the constraints from the jets+MET+zero-lepton search may be relaxed.

Gluon emission

The second case is that the gluino decays into a neutralino and a gluon via the top-stop loop process. The decay chain is $\tilde{g} \to gX_2 \to gZX_1$, as shown in Fig. 2b. Examples of this category include the mini-split SUSY [20–25] scenario [7]. If $X_2 \simeq \tilde{H}_u$, $X_1 \simeq \tilde{B}$ with compressed mass spectrum and heavy ($O(10^{1-3})$ TeV) squarks, the branching fraction of $\tilde{g} \to gX_2$ is enhanced and can be a dominant mode [26–28]. The branching fraction of $X_2 \to ZX_1$ is almost 100% if $M_Z < M_{X_2} - M_{X_1} < M_h$. Another example is a goldstini [29] scenario [8]. In this case, $X_2 \simeq \tilde{B}$ and $X_1 \simeq \tilde{G}'$, where $\tilde{G}'$ is a (massive) pseudo-goldstino. The small interactions of the pseudo-goldstino prevent the gluino directly decaying into the pseudo-goldstino. The branching fraction of $\tilde{g} \to gX_2$ is enhanced when the higgsinos and winos are significantly heavier than the bino. The branching fraction of $X_2 \to ZX_1$ can get to almost 100% if $M_Z < M_{X_2} - M_{X_1} < M_h$.

Decay into third generation squark

The third case is that the gluino decays into a squark lighter than it. From consideration of renormalization group equations, third generation squarks (stops and sbottoms) are likely to be light. The light sbottoms/stops scenario was considered in Ref. [9]. The stop/sbottom couples strongly to the higgsinos, so higgsino is taken as the NLSP and the bino is considered as the LSP. If the mass difference between the gluino and the stop/sbottom is small, the gluino mainly decays into the sbottom for kinematic reason. This decay chain $\tilde{g} \to b\tilde{b} \to b\bar{b}X_2 \to b\bar{b}ZX_1$, with $X_2 \simeq \tilde{H}_d$ and $X_1 \simeq \tilde{B}$, is shown in Fig. 2c. This scenario is severely constrained by b-jets search. For example, only a corner of parameter space (degenerate region) can marginally explain the ATLAS Z excess at 2σ level [9] while avoiding the ATLAS ≥ 3 b-jets + MET constraint [30].

2.2 Squark production

Our next category is the squark-pair production. This category is further divided according to the flavor of the squarks.

Squarks of the first and second generations

The first case is 1st/2nd generation squark production. Since 1st/2nd generation squarks produce less top and bottom quarks in their decay chains compared to the third generation, they are favored by various SUSY events searches. The decay chain is $\tilde{q} \to qX_2 \to qZX_1$, as shown in Fig. 2d. Examples are the NMSSM model with squark production [10] and the type of spectrum found by the dedicated parameter scan in pMSSM with 19 parameters [11]. In the former, $X_2 \simeq \tilde{B}$ and $X_1 \simeq \tilde{S}$ where $\tilde{S}$ is singlino. In the latter, $X_2 \simeq \tilde{B}$ and $X_1 \simeq \tilde{H}$. In this case, the branching fraction of the bino emitting a Z is not high and non-negligible amount of h and W are also produced.

Mixed stops

Stop pair production is also a possible case. However, since top quarks deposit characteristic signatures like (b-)jets, leptons, and/or missing energy, the stop decay mode $\tilde{t} \to t\tilde{\chi}$ is strongly disfavored. Actually, the branching fraction of $\tilde{t}_2 \to Z\tilde{t}_1$ can become dominant, if the above decay mode is kinematically forbidden (compressed case), or if left- and right-handed stops mix significantly (split case) [12]. As to the $\tilde{t}_1$ decay, assuming the decay mode $\tilde{t}_1 \to t\tilde{\chi}_1^0$ is kinematically forbidden, the dominant decay mode will be a flavor-violating two-body decay $\tilde{t}_1 \to q\tilde{\chi}_1^0$ (where $q = u, c$), or a flavor-conserving four-body decay $\tilde{t}_1 \to ff'b\tilde{\chi}_1^0$, where ff' are decay products of the off-shell W boson. Among the four combinations (compressed/split and flavor-conserving/violating), it was found in Ref. [12] that the flavor-violating compressed case best explains the ATLAS excess while circumventing other searches. Explicitly, the decay chain is $\tilde{t}_2 \to Z\tilde{t}_1 \to Zq\tilde{\chi}_1^0$, as shown in Fig. 2e. Another advantage of this decay chain is that it may explain the apparent discrepancy between ATLAS and CMS, since the Z boson is produced in the first step of the decay chain, and Jet Z Balance (JZB) distributes relatively symmetrically around 0 [12], which causes contamination in the CMS background. When we scan the parameter space in the following section, we extend the above flavor-violating compressed case to the flavor-violating split case, which has the same decay chain.

2.3 Non-SUSY model with a heavy gluon and vector-like quarks

The author of Ref. [13] considered an effective model whose particle contents are those of the Standard Model plus a heavy gluon G^* and vector-like quarks. It is realized in a composite Higgs model [31] or in a Randall-Sundrum model [32]. In this effective model, a pair of heavy quarks B_Z are produced via the G^* resonance, where B_Z has the same quantum numbers as the SM b quark and decays exclusively into b and Z boson. The decay chain is shown in Fig. 2f. Many parameters need to be fixed in such a way that constraints on the vector-like quarks are satisfied [13]. In addition, the mass of B_Z is also fixed at 930 GeV [13]. The remaining two relevant parameters are the light-heavy gluon mixing angle $\tan\theta_3$, and the mass of the heavy gluon M_{G^*}.

3 13 TeV LHC Test

3.1 Simulation Setup

To study the LHC signals and constraints on the various models discussed in section 2, we reduce them into simplified models by the following simplifications: (1) We take all the branching fractions

in the decay chains shown in Fig. 2 as 100% except that of the heavy gluon into a B_Z pair, which is far from 100% so we calculate it following Ref. [13]. Also, (2) we take all the irrelevant particles, *i.e.* particles not present in Fig. 2, as decoupled, except the first and second generation squark case (Fig. 2d), for which we consider both scenarios of decoupled gluino and 2.5 TeV gluino.

In our Monte Carlo simulation of the SUSY models, we generate the simplified models with up to one extra parton in the matrix element using MadGraph 5 v2.1.2 [33] interfaced to Pythia 6 [34] and Delphes 3 [35] (with FastJet incorporated [36]). We apply the MLM matching [37] with a scale parameter set to a quarter of the parent particle (gluino/squark) mass. The parton distribution functions (PDFs) from CTEQ6L1 [38] are used. The production cross sections are calculated at next-to-leading order (NLO) in the strong coupling constant, adding the resummation of soft gluon emission at next-to-leading-logarithmic accuracy (NLO+NLL) by using NLL-fast v2.1 (for 8 TeV) and v3.0 (for 13 TeV) [39]. For the non-SUSY model considered, we use FeynRules 2.3.13 [40] to write the Lagrangian, which is connected to MadGraph via the UFO interface [41]. The rest of the simulation set up is the same as for the SUSY models.

3.2 Relevant Experimental Searches

Our primary interest in this paper is the Z+MET excess. And we investigate five different Z+MET searches: "ATLAS8 Z+MET" [1], "ATLAS13 Z+MET" [15], "CMS8 Z+MET" [14], "CMS13 (ATLAS-like)" and "CMS13 (SRA-B)" [16]. It is useful to summarize and compare their cuts.

First, all of them share the same cut that there is at least one opposite sign same flavor (OSSF) dilepton pair (e^+e^- or $\mu^+\mu^-$) with on-Z invariant mass $81 < m_{ll} < 101$ GeV. Beyond this, the three searches ATLAS8 Z+MET, ATLAS13 Z+MET, and CMS13 (ATLAS-like) are very similar to each other. They all share the following cuts: large MET $E_{\rm T}^{\rm miss} > 225$ GeV, large hadronic activity $H_{\rm T} > 600$ GeV, at least two signal jets $n_{\rm jets} \geq 2$, and a minimum azimuthal separation between them and the missing momentum $\Delta\phi({\rm jet}_{12}, p_{\rm T}^{\rm miss}) > 0.4$ to suppress large fake MET events due to jet mismeasurement. The small differences among these three searches are primarily in the transverse momentum thresholds of lepton $p_{\rm T}^l$ and signal jet $p_{\rm T}^{\rm jet}$. Specifically, ATLAS8 Z+MET requires $p_{\rm T}^{l_1} > 25$ GeV, $p_{\rm T}^{l_2} > 10-14$ GeV depending on the trigger used, and $p_{\rm T}^{\rm jet} > 35$ GeV. ATLAS13 Z+MET requires $p_{\rm T}^{l_1} > 50$ GeV, $p_{\rm T}^{l_2} > 25$ GeV, and $p_{\rm T}^{\rm jet} > 30$ GeV. CMS13 (ATLAS-like) requires $p_{\rm T}^{l_1,l_2} > 20$ GeV, $p_{\rm T}^{\rm jet} > 35$ GeV, and also a minimum separation $\Delta R \equiv \sqrt{(\Delta\phi)^2 + (\Delta\eta)^2} > 0.1$ between the dilepton pair, where η is the pseudorapidity.

The other two searches, CMS8 Z+MET and CMS13 (SRA-B), are more different from the previous three. The CMS8 Z+MET search contains two inclusive signal regions: $n_{\rm jets} \geq 2$ and $n_{\rm jets} \geq 3$. Each signal region is further divided into three exclusive bins of $E_{\rm T}^{\rm miss}$: $100-200$, $200-300$, or > 300 GeV. Transverse momentum thresholds are $p_{\rm T}^{l_1,l_2} > 20$ GeV and $p_{\rm T}^{\rm jet} > 40$ GeV. A separation $\Delta R > 0.3$ between signal leptons is also required. The CMS13 (SRA-B) search contains two exclusive signal regions: $n_{\rm jets} = 2, 3$ (SRA) and $n_{\rm jets} \geq 4$ (SRB). SRA has a $H_{\rm T}$ cut $H_{\rm T} > 400 + p_{\rm T}^{l_1} + p_{\rm T}^{l_2}$ GeV, while SRB does not. Each of them is further divided into $2 \times 4 = 8$ exclusive bins according to $n_{b\text{-jets}}$: 0 or ≥ 1, and $E_{\rm T}^{\rm miss}$: $100-150$, $150-225$, $225-300$, or > 300 GeV. Transverse momentum thresholds and dilepton separation requirements are the same as CMS13 (ATLAS-like). A summary of these detailed comparisons is in Table 2.

The models discussed in section 2 typically have accompanying signal channels. In particular, the jets+MET+zero-lepton channel can often be quite constraining. Therefore, in addition to the five Z+MET searches above, we also investigate the constraints from "ATLAS8 jets+MET" search [42],

Table 2: Comparison of the cuts of Z+MET searches.

		$E_{\rm T}^{\rm miss}$	$H_{\rm T}$	$n_{\rm jets}$	$n_{b\text{-jets}}$	$\Delta\phi({\rm jet}_{12}, p_{\rm T}^{\rm miss})$	$p_{\rm T}^{l_1}$	$p_{\rm T}^{l_2}$	$p_{\rm T}^{\rm jet}$	ΔR
ATLAS8 Z+MET		> 225	> 600	≥ 2		> 0.4	> 25	$>$10-14	> 35	
ATLAS13 Z+MET							> 50	> 25	> 30	
CMS13 (ATLAS-like)							> 20	> 20	> 35	> 0.1
CMS8 Z+MET	$\geq$ 2j	100-200 200-300 > 300		≥ 2			> 20	> 20	> 40	> 0.3
	$\geq$ 3j			≥ 3						
CMS13 (SRA-B)	SRA	100-150 150-225 225-300 > 300	$> 400 + p_{\rm T}^{l_1} + p_{\rm T}^{l_2}$	2,3	0 ≥ 1		> 20	> 20	> 35	> 0.1
	SRB			≥ 4						

and "ATLAS13 jets+MET" search [43]. The four lepton searches [44, 45] require production of two Z bosons, both decaying leptonically. Therefore, these signatures strongly depend on the branching fraction of the parent particle into Z bosons, which is simplified to 100% in our simplified models except the non-SUSY model. Typically, the small leptonic branching fractions of the Z boson, ${\rm BF}_{\rm Zlep} = 6.7\%$ [46], makes the signal strength less significant. However, since these searches focus on small MET and jet activity events, even models with compressed spectrum and hence tiny Z+MET and multi-jet+MET acceptance rates, can be constrained by them. In our simplified models, the four lepton search signal strengths essentially depend on just the cross section of the parent particle $\sigma_{\rm parent}$, and the leptonic decay branching fraction of Z boson. Roughly speaking, $\sigma_{\rm parent} \times {\rm BF}^2_{{\rm parent}\to Z} \gtrsim 150$ fb, is excluded. One lepton searches [47, 48] are less important for the simplified models we consider, due to the second lepton veto cut.

3.3 Results

In this section, we list our simulation results of the models discussed in section 2. For each simplified model, we show the 1σ and 2σ fitting regions of the ATLAS8 Z+MET [1], and the 1σ fitting region of the ATLAS13 Z+MET [15]. To determine these fitting regions, we first estimate the visible cross sections, $(\epsilon\sigma)^{\rm NP}_{\rm 8TeV}$ for the 8 TeV case and $(\epsilon\sigma)^{\rm NP}_{\rm 13TeV}$ for the 13 TeV case. We estimate a χ^2 variable for the total number of the signal events, assuming the SM background uncertainty is Gaussian. We refer to the parameter regions where $\Delta\chi^2 < 1\,(4)$ as 1σ (2σ) fitting regions.

In addition to the fitting regions, we also show the 95% CL$_S$ exclusion curves from the ATLAS13 Z+MET [15], CMS8 Z+MET [14], CMS13 (ATLAS-like) and CMS13 (SRA-B) [16], ATLAS8 jets+MET [42], and ATLAS13 jets+MET [43].

3.3.1 SUSY GGM Models

In this category, we consider the SUSY GGM models, in which the LSP is the gravitino and massless. The parent particles are either a gluino pair or a squark pair, with the decay chain $\tilde{g} \to q\bar{q}({\rm NLSP} \to Z + {\rm LSP})$ (Fig. 2a) and $\tilde{q} \to q({\rm NLSP} \to Z + {\rm LSP})$ (Fig. 2d) respectively. For the gluino case, squarks are assumed to be very heavy and the gluino decays into four light flavor quarks (u, d, s, c). For the squark case, $\tilde{Q}_{L,12}$,$\tilde{u}_{r,12}$ and $\tilde{d}_{r,12}$ are light and have the common mass, and the gluino is assumed to be decoupled. We take the masses of the gluino/squark and the NLSP as free parameters.

The fitting regions and the exclusion bounds are shown in Fig. 3. We see that there is some

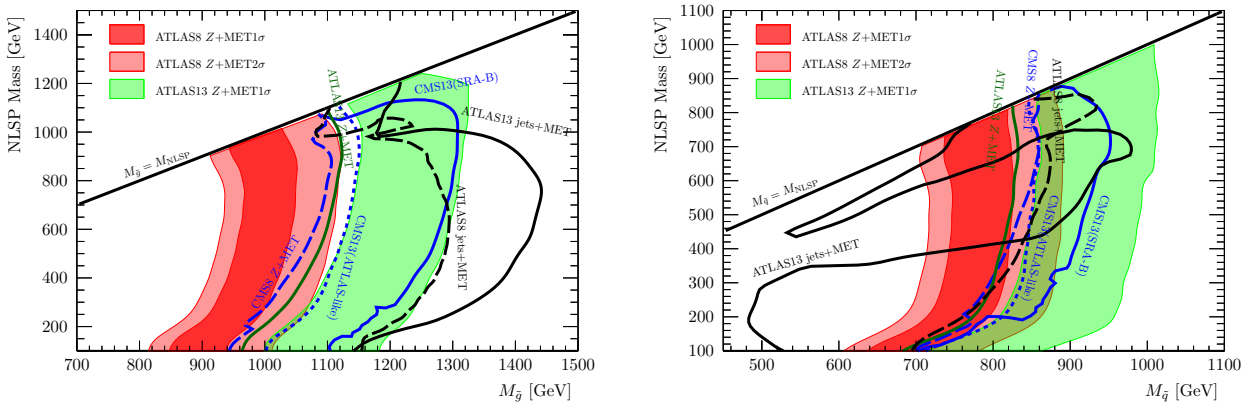

(a) GGM with gluino

(b) GGM with squark

Figure 3: 1σ and 2σ fitting regions of the ATLAS Z+MET excess and 95% exclusion bounds from various constraints for simplified GGM models: (a) gluino pair production with the decay chain $\tilde{g} \to q\bar{q}(\text{NLSP} \to Z + \text{LSP})$ (Fig. 2a), and (b) squark and anti-squark pair production with the decay chain $\tilde{q} \to q(\text{NLSP} \to Z + \text{LSP})$ (Fig. 2d). Four lepton searches excludes gluino (squark) mass up to about 800 (550) GeV.

tension between ATLAS8 Z+MET and ATLAS13 Z+MET fitting regions. In addition, the ATLAS jets+MET constraints are quite powerful and exclude a large portion of the fitting regions, especially in the case of gluino production. The CMS13 (SRA-B) constraint also excludes most of the fitting regions as expected. Four lepton searches excludes gluino (squark) mass up to about 800 (550) GeV.

3.3.2 Compressed SUSY Models

In this category, we consider the compressed SUSY models, in which the masses of the NLSP and the LSP are close. We study several scenarios according to different parent particles and decay chains.

Gluino pair production scenario

The first scenario we consider is the gluino pair production. The gluino decay chain is either a 3-body decay as shown in Fig. 2a, or a 2-body decay as shown in Fig. 2b. In the 3-body decay case, the gluino decays into four light flavor quarks (u, d, s, c). We fix the mass gap between the NLSP and the LSP as 100 GeV, and take the gluino mass and the LSP mass as free parameters.

The fitting regions and the exclusion bounds are shown in Fig. 4. We see that the ATLAS jets+MET constraints are less constraining compared to the GGM cases, and the degenerate regime of the fitting region (where the NLSP mass is close to the gluino mass) is consistent with the ATLAS jets+MET searches. Although the tension between ATLAS8 Z+MET and ATLAS13 Z+MET fitting regions is slightly better than the GGM cases, the ATLAS13 result already excludes 1σ fitting regions for the ATLAS8 excess. The CMS8/13 constraints have quite severe tension with the ATLAS8 excess. Four lepton searches exclude gluino mass up to 800 (700) GeV for light (heavy) LSP regions.

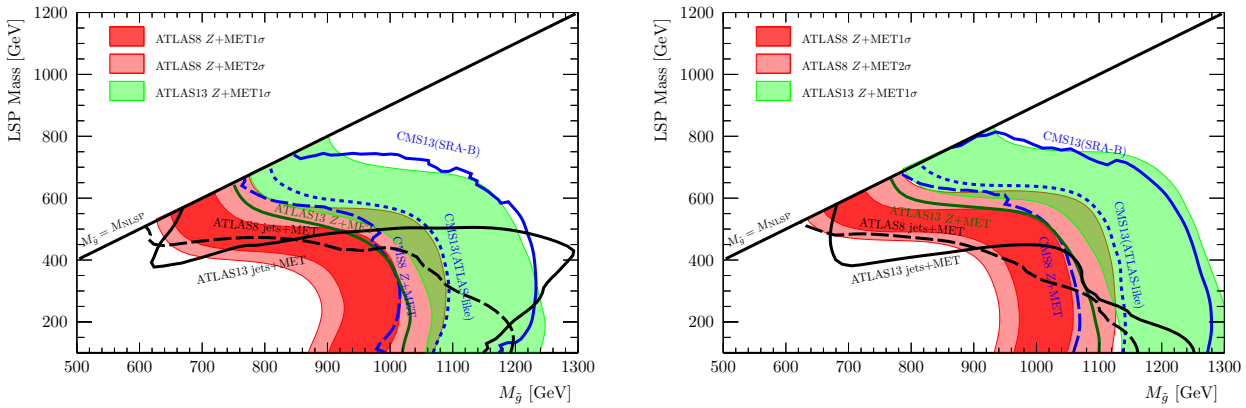

(a) Gluino 3-body

(b) Gluino 2-body

Figure 4: 1σ and 2σ fitting regions of the ATLAS Z+MET excess and 95% exclusion bounds from various constraints for simplified gluino pair production models: (a) gluino 3-body decay chain $\tilde{g} \to q\bar{q}(\text{NLSP} \to Z + \text{LSP})$ (Fig. 2a), and (b) gluino 2-body decay chain $\tilde{g} \to g(\text{NLSP} \to Z + \text{LSP})$ (Fig. 2b). Four lepton searches excludes gluino mass up to 800 (700) GeV for light (heavy) LSP regions.

Squark pair production scenario

We next consider the squark pair production scenario. For this scenario, the gluino mass is also an important parameter. If the gluino is extremely heavy or if the gluino has the Dirac mass term [49] and hence effectively decoupled, then squark-antisquark pair production through S-channel will dominate. On the other hand, if the gluino is relatively light, then squark-squark pair production through T-channel is dominant. Therefore, we consider two cases, one with decoupled gluino, the other with 2.5 TeV gluino. For each case, we fix the mass gap between the NLSP and the LSP as 100 GeV, and take the squark mass and the LSP mass as free parameters.

The fitting regions and the exclusion bounds are shown in Fig. 5. We see that similarly to the gluino production scenario, degenerate regime of the fitting region is consistent with the jets+MET searches. In addition, the tension between ATLAS8 Z+MET and ATLAS13 Z+MET fitting regions is also ameliorated. This is because the squarks with the decoupled gluino have smaller production cross section. On the other hand, the squarks with the light gluino are mainly produced by the valence quarks. In both cases, the R value tends to be small and leads to better consistency between the 8 TeV and 13 TeV ATLAS results. For the 2.5 TeV gluino case, a small portion of the fitting region is not excluded by the CMS Z+MET constraints. Four lepton searches exclude squark mass up to about 500 (800) GeV in the decoupled (2.5 TeV) gluino case.

Scenarios with light third generation squark

As discussed in section 2, some models with light third generation squark can also explain the ATLAS Z+MET excess. These include (1) a gluino pair production with the gluino decay via a light sbottom (Fig. 2c), and (2) a stop pair production in the mixed stop model (Fig. 2e). In scenario (1), we fix the mass gaps $M_{\rm NLSP} - M_{\rm LSP} = 100$ GeV, $M_{\tilde{b}} - M_{\rm NLSP} = 150$ GeV, and take the gluino mass and the LSP mass as free parameters. In scenario (2), we fix the mass gap between $\tilde{t}_1$ and the

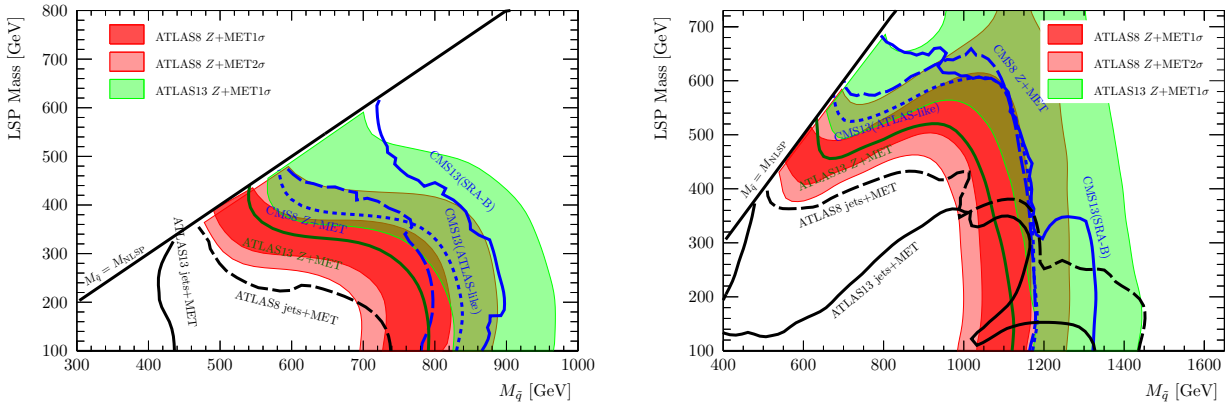

(a) squark with decoupled gluino

(b) squark with 2.5 TeV gluino

Figure 5: 1σ and 2σ fitting regions of the ATLAS Z+MET excess and 95% exclusion bounds from various constraints for simplified squark pair production models (Fig. 2d): (a) squark production with decoupled gluino, and (b) squark production with 2.5 TeV gluino. Four lepton searches exclude squark mass up to about 500 (800) GeV for case (a) ((b)).

LSP as 25 GeV, and take the masses of $\tilde{t}_2$ and the mass gap $\tilde{t}_2 - \tilde{t}_1$ as free parameters.

The fitting regions and the exclusion bounds are shown in Fig. 6. We see that the scenario (1) result is qualitatively similar to that of gluino 3-body decay scenario shown in Fig. 4a. This scenario is rich in b-jet signal, and hence subject to severe b-jet search constraints. Moreover, the present ATLAS 8 TeV excess does not prefer too many b-jets as seen in Table 1. If we take the b-jet number distribution into account, bulk of fitting region will be disfavored. For this simplified model, four lepton searches exclude gluino mass up to 750 GeV.

For scenario (2), the ATLAS8 Z+MET and ATLAS13 Z+MET fitting regions can be consistent, and the ATLAS jets+MET constraints are not severe. The CMS8 and 13 Z+MET constraints are significant. In this analysis, we adopt the background estimations provided by the ATLAS and CMS collaborations. However, as discussed in Ref. [12], the SUSY events in this model can contaminate the background estimations. In such cases, the tension between the CMS and ATLAS observations may be relaxed. For this simplified model, four lepton searches exclude $\tilde{t}_2$ mass up to 400 GeV.

3.3.3 Non-SUSY Model

For the non-SUSY model discussed in section 2, we fix the mass of B_Z at 930 GeV, and take the mass of the heavy gluon G^* and the mixing angle $\tan\theta_3$ as free parameters, following Ref. [13].

The fitting regions and the exclusion bounds are shown in Fig. 7. In the figure, the regions above the exclusion curves are excluded. In this analysis, we do not include the productions of the vector-like fermions other than B_Z nor the SM fermions through the heavy gluon. We see that the ATLAS jets+MET constraints and the CMS Z+MET constraints have relatively less tension with the fitting regions of the ATLAS excesses. This scenario is rich in energetic b-jet signal, and hence possibly subject to severe b-jet search constraints. Moreover, in this model, the momenta of the Z bosons are larger, since the Z bosons come from the heavy fermion decay $B_Z \to Zb$. Therefore it may conflict with the relatively low momenta of Z bosons in the signal region observed by ATLAS collaboration.

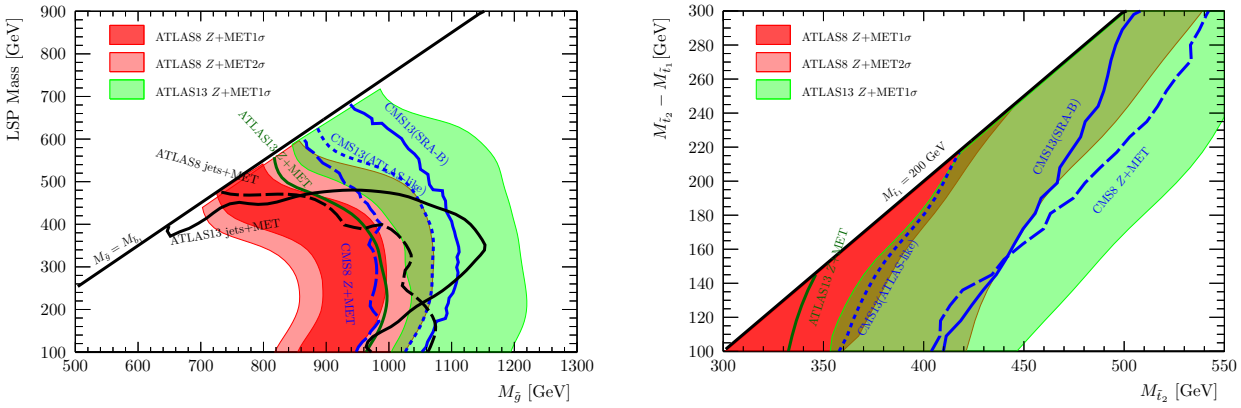

(a) gluino with light sbottom (b) mixed stop

Figure 6: 1σ and 2σ fitting regions of the ATLAS Z+MET excess and 95% exclusion bounds from various constraints for simplified models with light third generation squarks: (a) gluino pair production with decay via light sbottom (Fig. 2c), and (b) the mixed stop case with stop pair production (Fig. 2e). The constraint on the direct production of $\tilde{t}_1$ is $M_{\tilde{t}_1} \gtrsim 250$ GeV [50]. Four lepton searches exclude gluino($\tilde{t}_2$) mass up to 750 (400) GeV for case (a) ((b)).

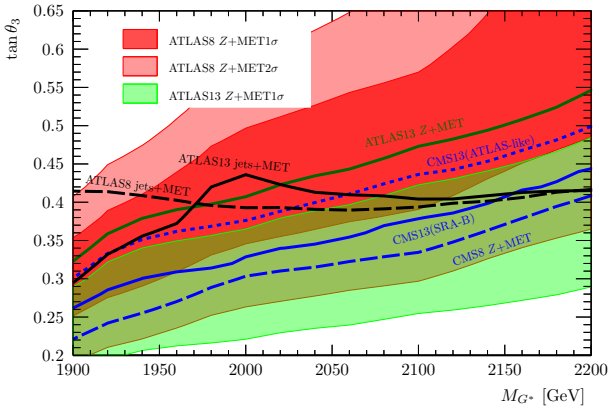

Figure 7: 1σ and 2σ fitting regions of the ATLAS Z+MET excess and 95% exclusion bounds from various constraints for simplified non-SUSY model with a heavy gluon and vector-like quarks (Fig. 2f).

3.4 Summary

Here we summarize the consistency of the ATLAS8 excess with the other LHC searches we considered.

vs Multi-jet+MET

If the mass difference between the parent particle and the LSP is large, ATLAS8/13 multi-jet+MET constraints conflict with the ATLAS8 Z+MET excess. On the other hand, if the mass spectrum is compressed, these constraints are weak and the current constraints from the 8/13 TeV running cannot exclude the ATLAS8 excess.

vs Z+MET by ATLAS13 and CMS13 ATLAS-like channel

Although ATLAS13 Z+MET search provides the 2.2σ excess, this can constrain some models. For instance, for the gluino production case, the best fit region for the ATLAS8 excess is excluded by the ATLAS13 result. This constraint is quite robust and almost independent of the details of the mass spectrum. The CMS13 ATLAS-like channel also provides a similar and slightly stronger constraint. This CMS13 constraint corresponds to $(\epsilon\sigma)^{\rm ATLAS}_{\rm 13TeV} \lesssim (4-5)$ fb in terms of the ATLAS13 event selection.

On the other hand, in the squark case, these constraints are not so severe. This is because the squark production cross section is relatively smaller than the gluino, and lighter squarks are favored to explain the ATLAS8 excess. In such a case, the enhancement of the cross section at the 13 TeV LHC is not so large and these constraints are relatively weaker. If the gluino mass is light enough to contribute to the squark production, the heavier squark mass is favored. In this case, however, the dominant production comes from valence quarks and the enhancement at the 13 TeV LHC is not so high. Therefore the Z+MET search by ATLAS13 and CMS13 ATLAS-like channel can be consistent with the ATLAS8 excess in the squark case.

This is also the case for the heavy gluon. Since the heavy gluon has spin 1, the dominant production channel is valence and sea quark fusion. Then the constraints of ATLAS13 and CMS13 get relatively weaker.

vs Z+MET by CMS8 and CMS13 SRA-B

Generally, compatibility between the ATLAS8 excess and the CMS8/13 constraints is hard. Regarding the CMS8 constraint, it uses different event selections from the ATLAS8 and the constraints are not parallel and model-dependent. This CMS8 constraint reads $(\epsilon\sigma)^{\rm ATLAS}_{\rm 8TeV} \lesssim (0.3-0.8)$ fb. This constraint excludes 1σ best fit region in many models.

The constraint by CMS13 SRA-B channel is also powerful to exclude the models. This constraint corresponds to $(\epsilon\sigma)^{\rm ATLAS}_{\rm 13TeV} \lesssim (1-5)$ fb. However this event selection is quite different from the ATLAS8/13 cut. Especially the b-jet multiplicity is important. For the Z+MET channel, one of the main SM background comes from $t\bar{t}$ events. In fact, in the SRB region, which requires ≥ 4 jets and provides best sensitivity for most of the models, the observed number of events with b-jets is about twice of without b-jets. Therefore the new physics models with b-jets suffer from relatively weaker constraints by the CMS13 SRA-B. The heavy gluon case is such an example as seen in Fig. 7. Therefore this constraint has larger model-dependence. For instance, allowing a small

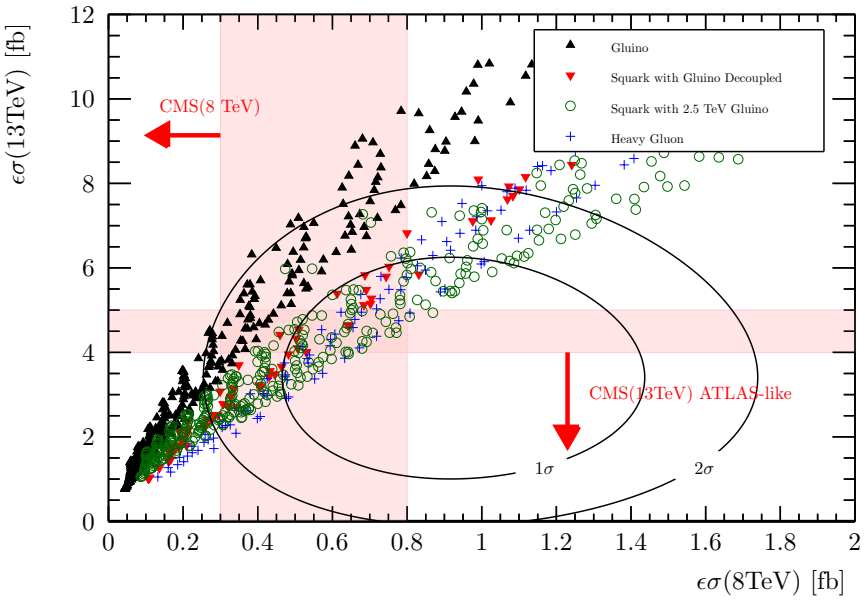

Figure 8: Scatter plot of the visible cross sections $\epsilon\sigma(8\text{ TeV})$ and $\epsilon\sigma(13\text{ TeV})$.

nonzero branching fraction into b quark may relax this constraint. In the case of the GGM with the gluino, we assume the gluino decay into u, d, s, and c quarks. In fact, by adding the b quark channel, we found the constraints get weaker. However in such a case, other multi-b jet searches will also constrain the models and thus the situation is complicated. Anyway, detailed analysis is out of the scope of the present simplified model.

In Fig. 8, we show a scatter plot of $\epsilon\sigma(8\text{ TeV})$ vs $\epsilon\sigma(13\text{ TeV})$ with favored regions in light of the ATLAS8/13 excesses. For reference, we show the constraints from CMS8 and CMS13(ATLAS-like) and its model dependence are shown in red shaded regions. For the gluino and squark cases, we adopt the degenerated mass spectrum and the gluino two body decay. We see that the new physics models capable to explain the ATLAS8 excess tend to predict larger cross sections at the 13 TeV LHC than observed. In particular, the gluino case predicts too large cross sections.

4 Discussion

After the ATLAS collaboration had reported the excess in the Z+MET excess in the 8 TeV LHC run, many new physics models were proposed. In this paper, we discussed the consistency of these models with the 8 TeV and 13 TeV LHC results. We found generally the 13 TeV LHC results give tension with the ATLAS8 excess.

Among new physics models, the squark case seems to provide relatively better fitting. In this paper, we assume 1st and 2nd generations and left and right-handed squarks have a common mass. If we remove this condition and assume, for instance, only right-handed squarks are light, the compatibility of the ATLAS8 excess fitting and other constraints will be improved, since the lighter squarks are preferred by the ATLAS8 excess and thus the R value gets smaller. Moreover, if we include the sbottom channel, the constraints by the 13 TeV LHC, particularly CMS13 SRA-B channel can be relaxed.

Although the squark cases provide better fittings, the constraints of ATLAS8/13 and CMS8/13 are not compatible completely. If the ATLAS8/13 excesses are true, the CMS8/13 searches would naturally have found some excesses. This incompatibility problem is most severe in between the ATLAS13 and CMS13 (ATLAS-like) searches, since these two essentially have the same event selection cuts. In fact, the observed numbers of total events for ATLAS13 and CMS13 seem to be consistent with each other. However, the background estimations look different. Therefore it would be possible that the incompatibility of the ATLAS8/13 and CMS8/13 Z+MET searches can come from the systematic difference of the SM background estimations. We hope the ATLAS and CMS collaborations investigate the compatibility of the background estimations of both collaborations and reveal the origin of the deviation.

Finally let us comment on the uncertainty of our signal estimations. For the consistency between the ATLAS Z+MET and multi-jet+MET signals, we mainly focus on the compressed mass spectra. In such cases, however, the signal estimation suffers from larger uncertainties of the event generator and detector simulations although our simulation setup is calibrated so that we can reproduce the new physics constraints provided by the ATLAS and CMS papers. For instance, using different subversions of Pythia with default parameters, we found up to 50% difference in the acceptance rates at the same parameter point. These uncertainties give large impacts on the exclusion curves of the multi-jet+MET signals. For more accurate signal estimations, we need more careful treatment on these uncertainties. However, we expect these uncertainties give less impact on the Z+MET signals and our conclusion will be essentially unchanged.

Acknowledgments

XL is supported by DOE grant DE-SC-000999. TT acknowledges JSPS for a Grant-in-Aid for JSPS Fellows and the Grant-in-Aid for Scientific Research No. 26·10619.

References

[1] G. Aad *et al.* (ATLAS), Eur. Phys. J. **C75**, 318 (2015), [Erratum: Eur. Phys. J.C75,no.10,463(2015)], arXiv:1503.03290 [hep-ex].

[2] G. Barenboim, J. Bernabeu, V. A. Mitsou, E. Romero, E. Torro, and O. Vives, (2015), arXiv:1503.04184 [hep-ph]; V. A. Mitsou, in *4th International Conference on New Frontiers in Physics (ICNFP 2015) Kolymbari, Greece, August 23-30, 2015* (2015) arXiv:1512.06166 [hep-ph].

[3] B. Allanach, A. Raklev, and A. Kvellestad, Phys. Rev. **D91**, 095016 (2015), arXiv:1504.02752 [hep-ph].

[4] U. Ellwanger, Eur. Phys. J. **C75**, 367 (2015), arXiv:1504.02244 [hep-ph].

[5] J. Cao, L. Shang, J. M. Yang, and Y. Zhang, JHEP **06**, 152 (2015), arXiv:1504.07869 [hep-ph].

[6] K. Harigaya, M. Ibe, and T. Kitahara, (2015), arXiv:1510.07691 [hep-ph].

[7] X. Lu, S. Shirai, and T. Terada, JHEP **09**, 204 (2015), arXiv:1506.07161 [hep-ph].

[8] S. P. Liew, A. Mariotti, K. Mawatari, K. Sakurai, and M. Vereecken, Phys. Lett. **B750**, 539 (2015), arXiv:1506.08803 [hep-ph].

[9] A. Kobakhidze, N. Liu, L. Wu, and J. M. Yang, Phys. Rev. **D92**, 075008 (2015), arXiv:1504.04390 [hep-ph].

[10] J. Cao, L. Shang, J. M. Yang, and Y. Zhang, JHEP **10**, 178 (2015), arXiv:1507.08471 [hep-ph].

[11] M. Cahill-Rowley, J. L. Hewett, A. Ismail, and T. G. Rizzo, Phys. Rev. **D92**, 075029 (2015), arXiv:1506.05799 [hep-ph].

[12] J. H. Collins, J. A. Dror, and M. Farina, Phys. Rev. **D92**, 095022 (2015), arXiv:1508.02419 [hep-ph].

[13] N. Vignaroli, Phys. Rev. **D91**, 115009 (2015), arXiv:1504.01768 [hep-ph].

[14] V. Khachatryan *et al.* (CMS), JHEP **04**, 124 (2015), arXiv:1502.06031 [hep-ex].

[15] ATLAS Collaboration, ATLAS-CONF-2015-082 (2015).

[16] CMS Collaboration (CMS), CMS-PAS-SUS-15-011 (2015).

[17] M. Schreyer, A. Redelbach, and R. Strhmer, *Search for supersymmetry in events containing light leptons, jets and missing transverse momentum in* $\sqrt{s} = 8TeVpp$ *collisions with the ATLAS detector*, Ph.D. thesis, Wurzburg U. (2015), presented 25 Sep 2015.

[18] P. Meade, N. Seiberg, and D. Shih, Prog. Theor. Phys. Suppl. **177**, 143 (2009), arXiv:0801.3278 [hep-ph].

[19] M. Buican, P. Meade, N. Seiberg, and D. Shih, JHEP **03**, 016 (2009), arXiv:0812.3668 [hep-ph].

[20] J. D. Wells, (2003), arXiv:hep-ph/0306127 [hep-ph]; J. D. Wells, Phys.Rev. **D71**, 015013 (2005), arXiv:hep-ph/0411041 [hep-ph].

[21] N. Arkani-Hamed and S. Dimopoulos, JHEP **0506**, 073 (2005), arXiv:hep-th/0405159 [hep-th]; G. Giudice and A. Romanino, Nucl.Phys. **B699**, 65 (2004), arXiv:hep-ph/0406088 [hep-ph]; N. Arkani-Hamed, S. Dimopoulos, G. Giudice, and A. Romanino, Nucl.Phys. **B709**, 3 (2005), arXiv:hep-ph/0409232 [hep-ph].

[22] L. J. Hall and Y. Nomura, JHEP **1201**, 082 (2012), arXiv:1111.4519 [hep-ph]; L. J. Hall, Y. Nomura, and S. Shirai, JHEP **1301**, 036 (2013), arXiv:1210.2395 [hep-ph]; Y. Nomura and S. Shirai, Phys.Rev.Lett. **113**, 111801 (2014), arXiv:1407.3785 [hep-ph].

[23] M. Ibe and T. T. Yanagida, Phys.Lett. **B709**, 374 (2012), arXiv:1112.2462 [hep-ph]; M. Ibe, S. Matsumoto, and T. T. Yanagida, Phys.Rev. **D85**, 095011 (2012), arXiv:1202.2253 [hep-ph].

[24] A. Arvanitaki, N. Craig, S. Dimopoulos, and G. Villadoro, JHEP **1302**, 126 (2013), arXiv:1210.0555 [hep-ph].

[25] N. Arkani-Hamed, A. Gupta, D. E. Kaplan, N. Weiner, and T. Zorawski, (2012), arXiv:1212.6971 [hep-ph].

[26] M. Toharia and J. D. Wells, JHEP **0602**, 015 (2006), arXiv:hep-ph/0503175 [hep-ph].

[27] P. Gambino, G. Giudice, and P. Slavich, Nucl.Phys. **B726**, 35 (2005), arXiv:hep-ph/0506214 [hep-ph].

[28] R. Sato, S. Shirai, and K. Tobioka, JHEP **1211**, 041 (2012), arXiv:1207.3608 [hep-ph]; R. Sato, S. Shirai, and K. Tobioka, JHEP **1310**, 157 (2013), arXiv:1307.7144 [hep-ph].

[29] C. Cheung, Y. Nomura, and J. Thaler, JHEP **03**, 073 (2010), arXiv:1002.1967 [hep-ph].

[30] G. Aad *et al.* (ATLAS), JHEP **10**, 24 (2014), arXiv:1407.0600 [hep-ex].

[31] D. B. Kaplan and H. Georgi, Phys. Lett. **B136**, 183 (1984).

[32] L. Randall and R. Sundrum, Phys. Rev. Lett. **83**, 3370 (1999), arXiv:hep-ph/9905221 [hep-ph].

[33] J. Alwall, R. Frederix, S. Frixione, V. Hirschi, F. Maltoni, *et al.*, JHEP **1407**, 079 (2014), arXiv:1405.0301 [hep-ph]; J. Alwall, M. Herquet, F. Maltoni, O. Mattelaer, and T. Stelzer, JHEP **1106**, 128 (2011), arXiv:1106.0522 [hep-ph].

[34] T. Sjostrand, S. Mrenna, and P. Z. Skands, JHEP **0605**, 026 (2006), arXiv:hep-ph/0603175 [hep-ph].

[35] J. de Favereau *et al.* (DELPHES 3), JHEP **1402**, 057 (2014), arXiv:1307.6346 [hep-ex].

[36] M. Cacciari, G. P. Salam, and G. Soyez, Eur.Phys.J. **C72**, 1896 (2012), arXiv:1111.6097 [hep-ph]; M. Cacciari and G. P. Salam, Phys.Lett. **B641**, 57 (2006), arXiv:hep-ph/0512210 [hep-ph].

[37] J. Alwall, S. Hoche, F. Krauss, N. Lavesson, L. Lonnblad, *et al.*, Eur.Phys.J. **C53**, 473 (2008), arXiv:0706.2569 [hep-ph].

[38] J. Pumplin, D. Stump, J. Huston, H. Lai, P. M. Nadolsky, *et al.*, JHEP **0207**, 012 (2002), arXiv:hep-ph/0201195 [hep-ph].

[39] W. Beenakker, R. Hopker, M. Spira, and P. Zerwas, Nucl.Phys. **B492**, 51 (1997), arXiv:hep-ph/9610490 [hep-ph]; A. Kulesza and L. Motyka, Phys.Rev.Lett. **102**, 111802 (2009), arXiv:0807.2405 [hep-ph]; A. Kulesza and L. Motyka, Phys.Rev. **D80**, 095004 (2009), arXiv:0905.4749 [hep-ph]; W. Beenakker, S. Brensing, M. Kramer, A. Kulesza, E. Laenen, *et al.*, JHEP **0912**, 041 (2009), arXiv:0909.4418 [hep-ph]; W. Beenakker, S. Brensing, M. Kramer, A. Kulesza, E. Laenen, *et al.*, Int.J.Mod.Phys. **A26**, 2637 (2011), arXiv:1105.1110 [hep-ph]; W. Beenakker, M. Kramer, T. Plehn, M. Spira, and P. M. Zerwas, Nucl. Phys. **B515**, 3 (1998), arXiv:hep-ph/9710451 [hep-ph]; W. Beenakker, S. Brensing, M. Kramer, A. Kulesza, E. Laenen, and I. Niessen, JHEP **08**, 098 (2010), arXiv:1006.4771 [hep-ph].

[40] A. Alloul, N. D. Christensen, C. Degrande, C. Duhr, and B. Fuks, Comput. Phys. Commun. **185**, 2250 (2014), arXiv:1310.1921 [hep-ph].

[41] C. Degrande, C. Duhr, B. Fuks, D. Grellscheid, O. Mattelaer, and T. Reiter, Comput. Phys. Commun. **183**, 1201 (2012), arXiv:1108.2040 [hep-ph].

[42] G. Aad *et al.* (ATLAS), JHEP **1409**, 176 (2014), arXiv:1405.7875 [hep-ex].

[43] ATLAS Collaboration, ATLAS-CONF-2015-062 (2015).

[44] G. Aad *et al.* (ATLAS), Phys. Rev. **D90**, 052001 (2014), arXiv:1405.5086 [hep-ex].

[45] S. Chatrchyan *et al.* (CMS), Phys. Rev. **D90**, 032006 (2014), arXiv:1404.5801 [hep-ex].

[46] K.A. Olive *et al.* (Particle Data Group), Chin. Phys. C **38**, 090001 (2014), and 2015 update.

[47] G. Aad *et al.* (ATLAS), JHEP **04**, 116 (2015), arXiv:1501.03555 [hep-ex].

[48] ATLAS collaboration, ATLAS-CONF-2015-076 (2015).

[49] R. Ding, Y. Fan, J. Li, T. Li, and B. Zhu, (2015), arXiv:1508.07452 [hep-ph].

[50] G. Aad *et al.* (ATLAS), Phys. Rev. **D90**, 052008 (2014), arXiv:1407.0608 [hep-ex].